BOLETÍN DE LA SOCIEDAD ESPAÑOLA DE CERÁMICA Y VIDRIO 60 (2021) 266–272

ELSEVIER

BOLETIN DE LA SOCIEDAD ESPAÑOLA DE
Cerámica y Vidrio
www.elsevier.es/bsecv

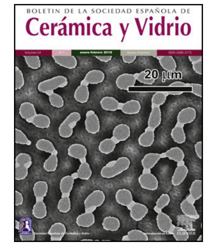

Original

Effect of antimony content on electrical and structural properties of $0.98(K_{0.48}Na_{0.52})_{0.95}Li_{0.05}Nb_{1-x}Sb_xO_3$–$0.02Ba_{0.5}(Bi_{0.5}Na_{0.5})_{0.5}ZrO_3$ ceramics

Brenda Carreño-Jiménez[a,*], *María Elena Villafuerte-Castrejón*[b], *Armando Reyes-Montero*[c], *Rigoberto López-Juárez*[a,*]

[a] *Unidad Morelia del Instituto de Investigaciones en Materiales, Universidad Nacional Autónoma de México, Antigua Carretera a Pátzcuaro No. 8701, Col. Ex Hacienda de San José de la Huerta, C.P. 58190 Morelia, Michoacán, Mexico*
[b] *Instituto de Investigaciones en Materiales, Universidad Nacional Autónoma de México, Ciudad Universitaria, A.P. 70-360, C.P. 04510 CDMX, Mexico*
[c] *Instituto de Ciencias Aplicadas y Tecnología, UNAM, Circuito Exterior s/n CU, México, D.F. 04510, Mexico*

ARTICLE INFO

Article history:
Received 4 March 2020
Accepted 1 June 2020
Available online 16 June 2020

Keywords:
KNN-based ceramics
Phase coexistence
Piezoelectric properties
Dielectric constant

ABSTRACT

Lead-free $0.98(K_{0.48}Na_{0.52})_{0.95}Li_{0.05}Nb_{1-x}Sb_xO_3$–$0.02Ba_{0.5}(Bi_{0.5}Na_{0.5})_{0.5}ZrO_3$ (KNLNS$_x$–BBNZ) solid solution with $0.04 < x < 0.08$ was prepared by traditional solid-state process. Samples were sintered using a conventional method at 1120 °C for 4 h. The effect of Sb^{5+} content on the phase structure, microstructure, ferroelectric, dielectric and piezoelectric properties of the KNLNS$_x$–BBNZ ceramics was studied. The phase transition of the ceramic was determined by the temperature dependence of the dielectric properties, while the structural properties, like the phase coexistence, were studied by X-ray diffraction. It was found that ceramics in the composition range of $0.06 < x < 0.08$ possess an orthorhombic (*Amm2*) and tetragonal (*P4mm*) phases coexistence. The best piezoelectric properties were obtained in the ceramics with $x = 0.07$: $d_{33} = 282$ pC/N, $-d_{31} = 103$ pC/N, $k_p = 46\%$, $\varepsilon_r = 1820$, $\tan\delta = 3\%$ and $T_c = 271$ °C. Furthermore, this composition exhibited a good thermal stability, up to 200 °C on d_{33} piezoelectric constant, indicating that this material have great potential for application from room temperature until this temperature limit.

* *Corresponding authors.*
E-mail addresses: bcarrenojimenez@gmail.com (B. Carreño-Jiménez), rlopez@iim.unam.mx (R. López-Juárez).
https://doi.org/10.1016/j.bsecv.2020.06.001

Efecto del contenido de antimonio en las propiedades eléctricas y estructurales de materiales cerámicos $0.98(K_{0.48}Na_{0.52})_{0.95}Li_{0.05}Nb_{1-x}Sb_xO_3$-$0.02Ba_{0.5}(Bi_{0.5}Na_{0.5})_{0.5}ZrO_3$

Palabras clave:
Materiales cerámicos con base en KNN
Coexistencia de fases
Propiedades piezoeléctricas
Constante dieléctrica

R E S U M E N

La solución sólida libre de plomo $0.98(K_{0.48}Na_{0.52})_{0.95}Li_{0.05}Nb_{1-x}Sb_xO_3$-$0.02Ba_{0.5}(Bi_{0.5}Na_{0.5})_{0.5}ZrO_3$ (KNLNS$_x$-BBNZ) con $0.04 < x < 0.08$ fue sintetizada por el método tradicional de estado sólido. Las muestras se sinterizaron a 1120 °C durante 4 horas. Se estudió el efecto del contenido de Sb^{5+} en las propiedades estructurales, microestructurales, ferroeléctricas, dieléctricas y piezoeléctricas de las cerámicas KNLNS$_x$-BBNZ. La transición de fase de los materiales cerámicos se determinó mediante la dependencia de las propiedades dieléctricas con respecto a la temperatura, mientras que las propiedades estructurales, como la coexistencia de fase, se estudiaron mediante difracción de rayos X. Se encontró que los materiales cerámicos con composición entre $0.06 < x < 0.08$ muestran una coexistencia de fases ortorrómbica *(Amm2)* y tetragonal *(P4mm)* (O-T). Las cerámicas con la composición $x = 0.07$ presentaron las mejores propiedades: $d_{33} = 282$ pC/N, $-d_{31} = 103$ pC/N, $k_p = 46\%$, $\varepsilon_r = 1820$, $\tan\delta = 3\%$ y $T_c = 271$ °C. Además, se observó una buena estabilidad térmica de la propiedad piezoeléctrica (d_{33}), hasta 200 °C, indicando un gran potencial en aplicaciones hasta este límite de temperatura.

Introduction

$K_{0.5}Na_{0.5}NbO_3$ (KNN) is one of the most promising lead-free solid solution in the realm of piezoelectric materials due its high Curie temperature (T_C). The study of its structural and dielectric properties shows the phase transition temperature of the rhombohedral-orthorhombic at −160 °C ($T_{R\text{-}O}$), orthorhombic-tetragonal at 200 °C ($T_{O\text{-}T}$) and tetragonal-cubic at 420 °C (T_C), while values of the piezoelectric parameters (d_{33}, d_{31} and k_p) are 80–120 pC/N, 30–40 pC/N and 0.24–0.40, respectively [1,2].

However, the piezoelectric properties of KNN and related materials are not as good as the currently commercial compounds due to the evaporation of alkali metals, which make it difficult to obtain a pure phase and a high densification of materials. Then, it has been proposed to add different substituents to promote the stability over the alkali metals and increase the electrical characteristics [3].

One way to improve the properties of KNN-based ceramics has been to imitate the structural characteristics of $Pb(Zr,Ti)O_3$ (PZT) [4]. That is, to shift the transition temperature of the ferroelectric phases (rhombohedral-orthorhombic and orthorhombic-tetragonal) toward room temperature. In order to achieve this shift in the phase transition, some substituents that have been proposed are Li^{1+} [5,6], Sb^{5+} [7,8], Ta^{5+} [9,10], $BiNaTiO_3$ [11], $BiFeO_3$ [12], $BiLiZrO_3$ [13], $BaCaTiZrO_3$ [14], $BaZrO_3$ [15,16] and $BiNaZrO_3$ [17].

Moreover, some studies with dopants like $Ca_{0.5}(Bi_{0.5}Na_{0.5})_{0.5}ZrO_3$ [18], $Sr_{0.5}(Bi_{0.5}Na_{0.5})_{0.5}ZrO_3$ [19] or $Ba_{0.5}(Bi_{0.5}Na_{0.5})_{0.5}ZrO_3$ [20], show a shift over a rhombohedral-tetragonal phase coexistence at room temperature.

Different reports show that antimony increases $T_{R\text{-}O}$ and decreases $T_{O\text{-}T}$ toward room temperature, causing an enhancing of the electrical properties [7,21,22]. However, it has been observed that the addition of antimony greater than 0.1 mol-fraction causes segregation, which decreases the electrical properties. Therefore, in this work the study of the KNLNS$_x$–BBNZ solid solution (where $x = 0.04$, 0.05, 0.055, 0.06, 0.065, 0.07 and 0.08) is proposed, to complement our recently research [20] and to analyze the effect of antimony on structural, microstructural and electrical properties of the proposed materials.

Experimental

Lead-free $0.98[(K_{0.48}Na_{0.52})_{0.95}Li_{0.05}Nb_{1-x}Sb_xO_3]$–$0.02[Ba_{0.5}(Bi_{0.5}Na_{0.5})_{0.5}ZrO_3]$ (KNLNS$_x$–BBNZ) ($x = 0.04$, 0.05, 0.055, 0.06, 0.065, 0.07 and 0.08) ceramics were prepared by conventional solid-state method. The starting materials used were Na_2CO_3 (Merck, 99.9%), Li_2CO_3 (Sigma–Aldrich, 99.99%), K_2CO_3 (JT Baker, 99.8%), $BaCO_3$ (Sigma–Aldrich, 99%), Nb_2O_5 (Sigma–Aldrich, 99.99%), ZrO_2 (Sigma–Aldrich, 99%), Bi_2O_3 (Sigma–Aldrich, 99.9%) and Sb_2O_5 (Sigma–Aldrich, 99.99%). After weighing, the reagents were mixed with acetone in an agate mortar for 30 min and dried. Then, the mixture was calcined at 850 °C for 3 h in air. Later, calcined powders were ball milled for 12 h. After that, the calcined powders were uniaxially pressed at 260 MPa into disks (13 mm diameter and 2 mm thickness) and sintered at 1120 °C for 4 h. Before measuring electrical properties, both major surfaces were coated with silver paste of the sintered disks and fired at 600 °C for 30 min. Afterwards, the disks were poled at room temperature for 30 min under a 4 kV/mm dc electric field.

The structural analysis of the ceramics was performed by X-ray diffraction (XRD) using a Bruker D2 Phaser diffractometer (CuK-α, $\lambda = 1.5406$ Å). The scanning electron microscopy (SEM) (JEOL-J7600F) was used to characterize the microstructure. An impedance analyzer (Agilent 4294A) was used to

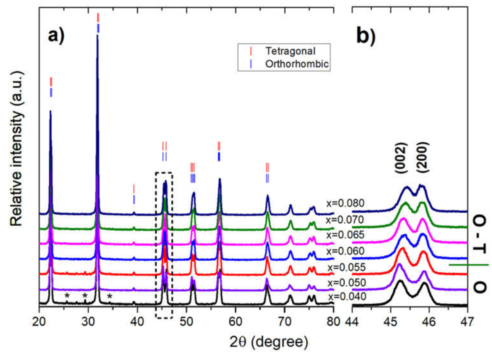

Fig. 1 – XRD patterns of $KNLNS_x$–BBNZ ceramics measured at (a) $2\theta = 20°–80°$; (b) zoom in the 44–47° 2θ range.

measure temperature dependence of the relative dielectric permittivity. The ferroelectric RT66B workstation was used to acquire the hysteresis loops of the ceramics. The electromechanical coupling factor (k_p) and radial piezoelectric constant (d_{31}) were determined by an iterative method [23], while the d_{33} was measured by Piezo Meter System (Piezotest, Inc.).

Results and discussion

Fig. 1(a) shows the X-ray diffraction (XRD) patterns of $KNLNS_x$–BBNZ ceramics measured at $2\theta = 20–80°$. A pure perovskite phase was observed in ceramics with $0.055 < x < 0.08$ without any other phases, indicating the formation of a solid solution. In compositions with $x = 0.04$, 0.05 and 0.055 a secondary phase was identified which corresponds to $K_3Li_2Nb_5O_{15}$, as shows in other reports [24], [25]. In order to clarify the phase evolution under different Sb^{5+} contents, the XRD were amplified in the 44–47° 2θ range and are shown in Fig. 1(b). It is clearly seen a progressive change in the relative intensity. First, a splitting of (022)/(200) peaks with different intensities are observed for $x \leq 0.055$, characteristic of orthorhombic phase; which change to (002)/(200) reflections with same intensities, characteristics of tetragonal-orthorhombic phase coexistence. Particularly, the intensity of (002) decreases while the (200) increases as x increases. The samples with x = 0.04, 0.05 and 0.055 shows an orthorhombic phase (O), (*Amm2*) [18,26]. For the $0.06 \leq x \leq 0.08$ compositions the phase structure changes to an orthorhombic-tetragonal phase coexistence (O-T), (*Amm2-P4mm*), as the amount of Sb^{5+} increases [27].

Our current research compared with other similar solid solutions and with our latest KNN-based study, shows that varying antimony content promotes different phase coexistence at room temperature, of rhombohedral-tetragonal to orthorhombic-tetragonal [18]. In addition, the structural characteristics are dependent on sintering temperature [7], since the sintered samples with $x = 0.05$ at 1135 °C for 4 h show a rhombohedral–tetragonal polymorphic phase transition (PPT) at room temperature [20], while Fig. 1(b) shows that sample sintered at 1120 °C show a single orthorhombic phase.

Scanning electron microscopy (SEM) was performed to study the microstructural evolution according to the Sb^{5+} incorporation on $KNLNS_x$–BBNZ ceramics. The grains have a cubic-like shape in all compositions, which is characteristic of the KNN-based ceramics (Fig. 2a–d), and the samples exhibit irregularly arranged large and small grains.

The average grain size was determined from the size distribution showed as an insert in SEM images that was measured using ImageJ with a linear method. Likewise, all

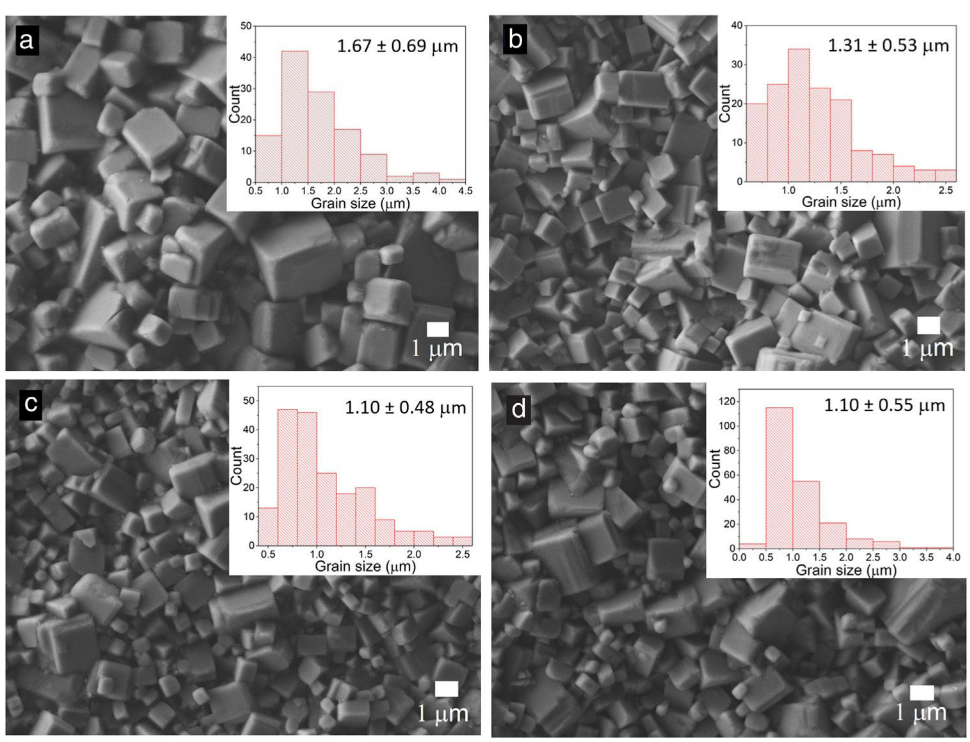

Fig. 2 – SEM micrographs of $KNLNS_x$–BBNZ sintered ceramic with x = (a) 0.05, (b) 0.06, (c) 0.07 and (d) 0.08.

samples exhibited a dense surface morphology, an important characteristic for enhancing the electrical properties of these materials.

The hysteresis loops measured at room temperature for KNLNS$_x$–BBNZ ceramics are presented in Fig. 3(a). All ceramics have hysteresis loops, characteristic of ferroelectric ceramics and are dependent on Sb^{5+} content. The remnant polarization (P_r) and the coercive field (E_C), as a function of Sb^{5+} content, are shown in Fig. 3(b). With the increment of Sb^{5+}, P_r and E_C increase and then dramatically drop at $x > 0.07$. The sample with $x = 0.07$ present the higher value in the remnant polarization, $P_r = 13.20\ \mu C/cm^2$.

The enhancement of ferroelectric properties at $x = 0.07$ should be the result of *O-T* phase coexistence, due that in the tetragonal phase there are 6 possible directions for polarization orientation, while there are 12 in the orthorhombic structure. Then, at phase coexistence, there exist 18 possibilities for polarization orientation.

The effect of Sb^{5+} content on the T_C values of KNLNS$_x$–BBNZ ceramics was also examined. Their relative dielectric permittivity (ε_r) versus temperature are shown in Fig. 4(a). The relative dielectric permittivity was measured from room temperature up to 500 °C (measured at 1 kHz), in order to include the T_C. The curves show a smooth peak close to room temperature, which can be assigned to the orthorhombic-tetragonal phase transition temperature ($T_{O\text{-}T}$) [8], [28]. The other peak is the T_C, where tetragonal-cubic phase transition occurs. T_C gradually decreases as the Sb^{5+} content increases beside the $T_{O\text{-}T}$ phase transition shifts to lower temperatures [7], [22]. Fig. 4(b) shows the ε_r at room temperature, and T_C values of the KNLNS$_x$–BBNZ ceramics, where the behavior of ε_r on T_C is depicted more clearly, and follow the tendency described

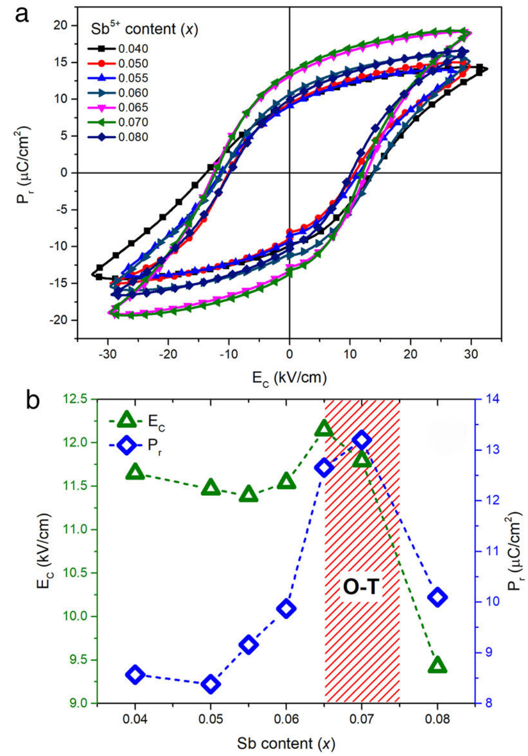

Fig. 3 – (a) Ferroelectric loop of the KNLNS$_x$–BBNZ ceramics; (b) P_r and E_c of the KNLNS$_x$–BBNZ ceramics as a function of x.

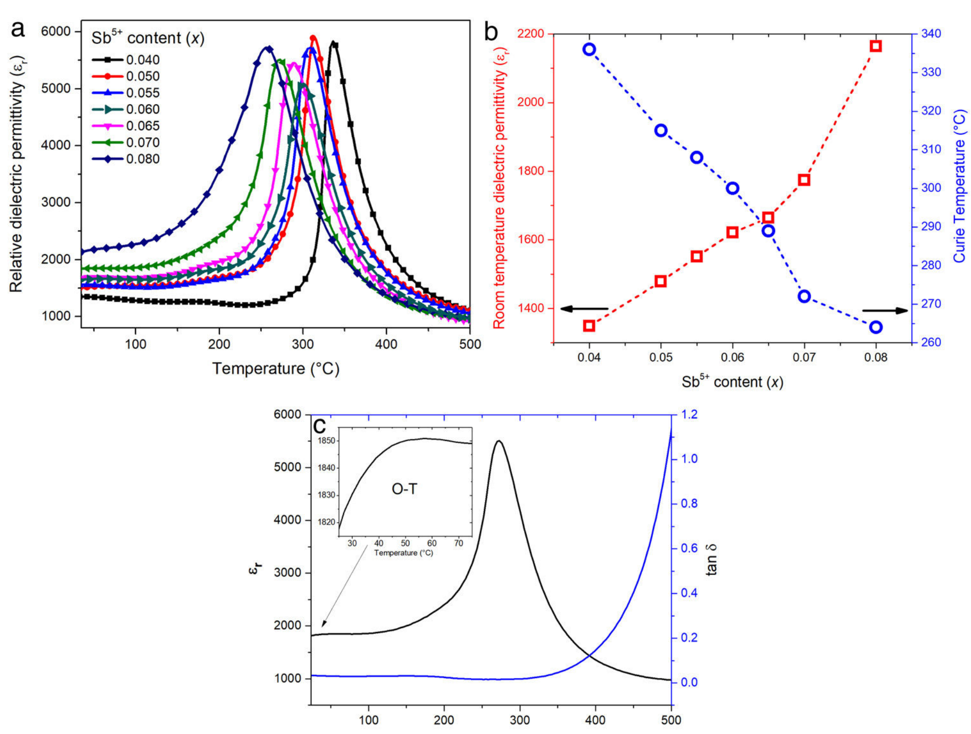

Fig. 4 – (a) Temperature dependence of the relative dielectric permittivity of KNLNS$_x$–BBNZ ceramics; (b) ε_r and T_C of KNLNS$_x$–BBNZ ceramics as a function of x; (c) temperature dependence of ε_r and tan δ of KNLNS$_x$–BBNZ with $x = 0.07$.

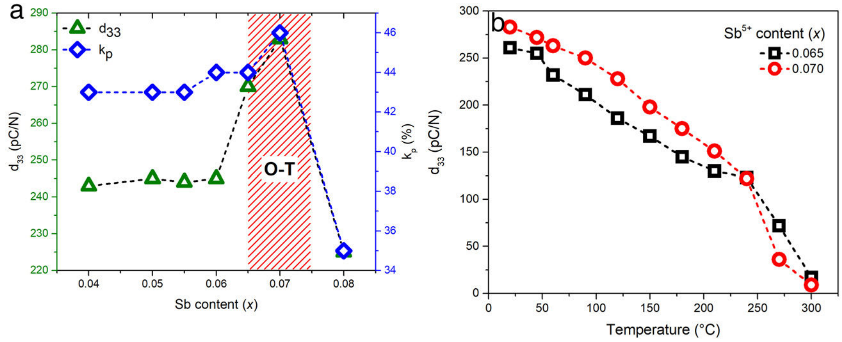

Fig. 5 – (a) d_{33} and k_p of KNLNS$_x$–BBNZ ceramics as a function of x; (b) d_{33} vs temperature of the ceramics KNLNS$_x$–BBNZ with x = 0.065 and 0.07.

Table 1 – Piezoelectric properties of KNLNS$_x$–BBNZ ceramics.

x (mol)	d_{33} (pC/N)	$-d_{31}$ (pC/N)	k_p (%)	g_{33} ($\times 10^{-2}$ vm/N)	S^E_{11} (10^{-2} m^2/N)	S^E_{12} (10^{-2} m^2/N)	S^E_{66} (10^{-2} m^2/N)	ε_{33}	$T\delta$
0.040	243	88.6 ± 4.4	44.0 ± 0.8	42	10.6 ± 0.2	−3.8 ± 0.1	28.9 ± 0.6	1348 ± 56	0.04
0.050	245	90.5 ± 3.3	44.2 ± 0.5	41	11.3 ± 0.2	−4.3 ± 0.1	31.2 ± 0.5	1351 ± 47	0.04
0.055	244	90.2 ± 3.9	43.1 ± 0.7	43	10.9 ± 0.2	−4.1 ± 0.1	30.0 ± 0.5	1464 ± 57	0.04
0.060	245	92.1 ± 4.0	43.5 ± 0.7	48	10.7 ± 0.2	−4.0 ± 0.1	29.5 ± 0.5	1505 ± 57	0.03
0.065	270	89.3 ± 4.2	40.7 ± 0.2	50	11.0 ± 0.2	−4.2 ± 0.1	30.3 ± 0.6	1594 ± 63	0.03
0.070	283	102.6 ± 5.0	45.9 ± 0.8	51	10.6 ± 0.2	−3.9 ± 0.1	29.0 ± 0.6	1692 ± 74	0.03
0.080	225	79.2 ± 4.5	35.4 ± 0.7	48	10.1 ± 0.2	−3.8 ± 0.1	27.9 ± 0.5	1788 ± 96	0.03

Table 2 – Electrical properties and phase coexistence at room temperature of KNN-based ceramics.

Composition	d_{33} (pC/N)	k_p (%)	T_C (°C)	Phase coexistence	Ref.
$K_{0.48}Na_{0.52}Nb_{0.93}Sb_{0.07}O_3$	∼225	42	–	R-O	[8]
$K_{0.47}Na_{0.47}Li_{0.06}Nb_{0.92}Sb_{0.08}O_3$	230	37	397	O-T	[29]
$K_{0.4}Na_{0.53}Li_{0.07}Nb_{0.91}Sb_{0.09}O_3$	∼290	∼48	∼310	O-T	[22]
$(K_{0.48}Na_{0.535})_{0.942}Li_{0.058}Nb_{0.94}Sb_{0.06}O_3$	298	34.5	∼300	O-T	[30]
$0.95K_{0.48}Na_{0.52}Nb_{0.97}Sb_{0.03}O_3$–$0.05Ca_{0.2}(Bi_{0.5}Na_{0.5})_{0.8}ZrO_3$	470	52.4	243	R-T	[31]
$0.97(K_{0.48}Na_{0.52})_{0.95}Li_{0.05}Nb_{0.94}Sb_{0.06}O_3$–$0.03Ca_{0.5}(Bi_{0.5}Na_{0.5})_{0.5}ZrO_3$	267	45.2	253	R-T	[18]
$0.98(K_{0.48}Na_{0.52})_{0.95}Li_{0.05}Nb_{0.93}Sb_{0.07}O_3$–$0.02Ba_{0.5}(Bi_{0.5}Na_{0.5})_{0.5}ZrO_3$	282	46	∼271	O-T	This work

before. Fig. 4(c) shows the relative dielectric permittivity (ε_r) and dielectric loss (tan δ) at 1 kHz of the composition at x = 0.07. The inset shows a zoom between 27 °C and 75 °C, where is observed the smooth peak mentioned in Fig. 4(a).

Fig. 5 (a) plots the d_{33} and k_p of KNLNS$_x$–BBNZ ceramics. Both parameters have a similar behavior, first an increase is shown and then drops at x > 0.07. The ceramics with x = 0.065 and 0.07 have the maximum piezoelectric values: d_{33} = 270 pC/N and 283 pC/N, respectively. The improvement of piezoelectric properties for these compositions can be ascribed to the phase coexistence mentioned above, due to the increment in polarization directions as well as higher permittivity. The summary of piezoelectric properties is shown in Table 1. The thermal stability of d_{33} is very important for the practical application, hence the stability of d_{33} in the ceramics with x = 0.065 and 0.07 was studied. These samples were exposed to heat treatment from room temperature to 300 °C for 1 h, cooled and the d_{33} measured. Fig. 5(b) shows a constant decline with the increase in temperature and then drops sharply when it approaches Curie temperature, both compounds have an abrupt loss of their piezoelectric properties after 240 °C, because they are close to paraelectric (cubic) phase and samples are losing their polarization.

For the sort of comparison, the piezoelectric properties for x = 0.07 are shown in Table 2, along with values reported in other investigations for similar compositions. The values of the piezoelectric parameters (d_{33} and k_p) in this work are of the same order of magnitude as those for the ceramic's compositions quoted in Table 1 and area superior to most of them due to the phase coexistence.

Conclusions

KNLNS$_x$–BBNZ lead-free piezoelectric ceramics were synthesized by conventional solid-state reaction method. These materials presented a cubic-like grain shape with crystal mean size close to 1 μm. From the XRD results, it was found that most compositions have pure perovskite phase, and at x = 0.07 it was found an orthorhombic-tetragonal phase coexistence. The Sb^{5+} content significantly affect phase structure and electrical properties. The O-T polymorphic phase transition enhanced the piezoelectric properties, i.e. d_{33}, d_{31} and k_p showed the highest values at $x = 0.07$, with $d_{33} = 282$ pC/N, $d_{31} = 103$ pC/N, $k_p = 46\%$, $\varepsilon_r = 1820$, $\tan\delta = 3\%$ and $T_c = 271\,^{\circ}C$. The excellent piezoelectric properties indicate that this composition might be a promising lead-free material for sensor and actuator application.

Funding

R. López-Juárez and M.E. Villafuerte-Castrejón gratefully acknowledge PAPIIT-UNAM for financial support under projects (IN113420) and (IN109018), respectively.

Conflict of interest

The authors reported no potential conflict of interest.

Acknowledgements

Brenda Carreño-Jiménez thanks to CONACyT-México for providing a PhD scholarship. The authors acknowledge to Omar Novelo (IIM-UNAM) for SEM images and Neftalí Razo (ENES-Morelia) for the technical assistance. A. Reyes-Montero acknowledges CTIC-UNAM for providing a post-doctoral scholarship.

REFERENCES

[1] Y. Saito, et al., Lead-free piezoceramics, Nature 432 (2004) 84–87.
[2] M. Ichiki, L. Zhang, M. Tanaka, R. Maeda, Electrical properties of piezoelectric sodium–potassium niobate, J. Eur. Ceram. Soc. 24 (6) (2004) 1693–1697.
[3] R. López-Juárez, R. Castañeda-Guzmán, M.E. Villafuerte-Castrejón, Fast synthesis of $NaNbO_3$ and $K_{0.5}Na_{0.5}NbO_3$ by microwave hydrothermal method, Ceram. Int. 40 (9) (2014) 14757–14764.
[4] E. Cross, Materials science: lead-free at last, Nature 432 (2004) 5–6.
[5] Z. Fu, J. Yang, P. Lu, L. Zhang, H. Yao, F. Xu, Influence of secondary phase on polymorphic phase transition in Li-doped KNN lead-free ceramics, Ceram. Int. 43 (15) (2017) 12893–12897.
[6] C. Long, et al., Li-substituted $K_{0.5}Na_{0.5}NbO_3$-based piezoelectric ceramics: crystal structures and the effect of atmosphere on electrical properties, J. Alloys Compd. 658 (2016) 839–847.
[7] J. Kim, J.H. Ji, D.J. Shin, J.H. Koh, Improved Li and Sb doped lead-free $(Na,K)NbO_3$ piezoelectric ceramics for energy harvesting applications, Ceram. Int. 44 (18) (2018) 22219–22224.
[8] J. Wu, H. Tao, Y. Yuan, X. Lv, X. Wang, X. Lou, Role of antimony in the phase structure and electrical properties of potassium–sodium niobate lead-free ceramics, RSC Adv. 5 (19) (2015) 14575–14583.
[9] R. Gao, X. Chu, Y. Huan, X. Wang, L. Li, $(K,Na)NbO_3$ based piezoceramics prepared by a two-step calcining and ball milling route, Mater. Lett. 123 (2014) 242–245.
[10] Y. Zhao, Y. Zhao, R. Huang, R. Liu, H. Zhou, Influence of B-site non-stoichiometry on structure and electrical properties of KNLNS lead-free piezoelectric ceramics, Mater. Lett. 75 (2012) 146–148.
[11] L. Liu, et al., Average vs. local structure and composition-property phase diagram of $K_{0.5}Na_{0.5}NbO_3$–$Bi_{1/2}Na_{1/2}TiO_3$ system, J. Eur. Ceram. Soc. 37 (4) (2017) 1387–1399.
[12] B. Wu, J. Ma, W. Wu, M. Chen, Y.X. Ding, $BiFeO_3$-modified $(K,Na,Li)(Nb,Sb)O_3$ lead free ceramics with high Curie temperature, J. Alloys Compd. 710 (2017) 130–137.
[13] B. Wu, J. Ma, W. Wu, M. Chen, Y. Ding, Enhanced electrical properties, phase structure, and temperature-stable dielectric of $(K_{0.48}Na_{0.52})NbO_3$-$Bi_{0.5}Li_{0.5}ZrO_3$ ceramics, Ceram. Int. 44 (1) (2018) 1172–1175.
[14] C. Kornphom, T. Udeye, P. Thongbai, T. Bongkarn, Phase structures, PPT region and electrical properties of new lead-free KNLNTS–BCTZ ceramics fabricated via the solid-state combustion technique, Ceram. Int. 43 (2017) S182–S192.
[15] J. Luo, et al., Phase transition and piezoelectricity of $BaZrO_3$-modified $(K,Na)NbO_3$ lead-free piezoelectric thin films, J. Am. Ceram. Soc. (October) (2018), p.jace.16172.
[16] L. Liu, Y. Huang, Y. Li, M. Wu, L. Fang, Oxygen-vacancy-related high-temperature dielectric relaxation and electrical conduction in $0.95K0.5Na0.5NbO_3$–$0.05BaZrO_3$ ceramic, Phys. B: Phys. Condens. Matter. 407 (1) (2012) 136–139.
[17] X. Wang, et al., Phase structure, electrical properties, and stability of $0.96(K_{0.48}Na_{0.52})_{1-x}Li_xNbO_3$–$0.04Bi_{0.5}Na_{0.5}ZrO_3$ lead-free piezoceramics, Curr. Appl. Phys. (2014).
[18] K. Zhang, et al., Phase transition and piezoelectric properties of dense $(K_{0.48},Na_{0.52})_{0.95}Li_{0.05}Sb_xNb_{(1-x)}O_3$–$0.03Ca_{0.5}(Bi_{0.5},Na_{0.5})_{0.5}ZrO_3$ lead free ceramics, J. Alloys Compd. 664 (2016) 503–509.
[19] Y. Cheng, et al., Investigation of high piezoelectric properties of KNNSb-Sr_xBNZ ceramics, J. Alloys Compd. 815 (2020) 152252.
[20] B. Carreño-Jiménez, A. Reyes-Montero, M.E. Villafuerte-Castrejón, R. López-Juárez, Piezoelectric, dielectric and ferroelectric properties of $(1-x)(K_{0.48}Na_{0.52})_{0.95}Li_{0.05}Nb_{0.95}Sb_{0.05}O_3$–$xBa_{0.5}(Bi_{0.5}Na_{0.5})_{0.5}ZrO_3$ lead-free solid solution, J. Electron. Mater. 47 (10) (2018) 6053–6058.
[21] H. Li, W.Y. Shih, W.-H. Shih, Effect of antimony concentration on the crystalline structure, dielectric, and piezoelectric properties of $(Na_{0.5}K_{0.5})_{0.945}Li_{0.055}Nb_{1-x}Sb_xO_3$ solid solutions, J. Am. Ceram. Soc. 3072 (2007) 3070–3072.
[22] L. Zheng, J. Wang, Q. Wu, G. Zang, C. Wang, J. Du, Porperties of $(Na_{0.53}K_{0.4}Li_{0.07})Nb_{(1-x)}Sb_xO_3$ ceramics with lithium and antimony content, J. Alloys Compd. 487 (2009) 231–234.
[23] C. Alemany, A.M. González, L. Pardo, B. Jiménez, F. Carmona, J. Mendiofa, Automatic determination of complex constants of piezoelectric lossy materials in the radial mode, J. Phys. D: Appl. Phys. 28 (5) (1995) 945–956.
[24] T.A. Skidmore, S.J. Milne, Phase development during mixed-oxide processing of a $[Na_{0.5}K_{0.5}NbO_3]_{1-x}$–$[LiTaO_3]_x$ powder, J. Mater. Res. 22 (8) (2007) 2265–2272.
[25] J. Kim, J. Ji, D. Shin, J. Koh, Improved Li and Sb doped lead-free $(Na,K)NbO_3$ piezoelectric ceramics for energy harvesting applications, Ceram. Int. 44 (2018) 22219–22224.
[26] B. Orayech, A. Faik, G.A. Lo, O. Fabelo, J.M. Igartua, Mode-crystallography analysis of the crystal structures and the low- and high-temperature phase transition in $Na_{0.5}K_{0.5}NbO_3$, Appl. Crystallogr. 48 (2015) 318–333.
[27] S. Dwivedi, T. Pareek, S. Kumar, Structure, dielectric, and piezoelectric properties of $K_{0.5}Na_{0.5}NbO_3$-based lead-free ceramics, RSC Adv. 8 (2018) 24286–24296.
[28] H. Li, W.Y. Shih, W.-H. Shih, Effect of antimony concentration on the crystalline structure, dielectric, and piezoelectric

properties of $(Na_{0.5}K_{0.5})_{0.945}Li_{0.055}Nb_{1-x}Sb_xO_3$ solid solutions, J. Am. Ceram. Soc. 90 (10) (2007) 3070–3072.
[29] J. Li, Q. Sun, Characterization of $(Na_{0.47}K_{0.47}Li_{0.06})(Sb_xNb_{1-x})O_3$ ceramics prepared by molten salt synthesis method, Solid State Commun. 149 (15–16) (2009) 581–584.
[30] Q. Zhang, B.P. Zhang, H.T. Li, P.P. Shang, Effects of Sb content on electrical properties of lead-free piezoelectric $[(Na_{0.535}K_{0.480})_{0.942}Li_{0.058}](Nb_{1-x}Sb_x)O_3$ ceramics, J. Alloys Compd. 490 (1–2) (2010) 260–263.
[31] D. Pan, et al., Composition induced rhombohedral–tetragonal phase boundary and high piezoelectric activity in $(K_{0.48},Na_{0.52})$ $(Nb_{(1-x)}Sb_x)O_3$–$0.05Ca_{0.2}(Bi_{0.5},Na_{0.5})_{0.8}ZrO_3$ lead-free piezoelectric ceramics, Solid State Commun. 259 (800) (2017) 29–33.